Supplementary information

Sweet Graphene: Exfoliation of Graphite and Preparation of Glucose-Graphene Cocrystals through Mechanochemical Treatments

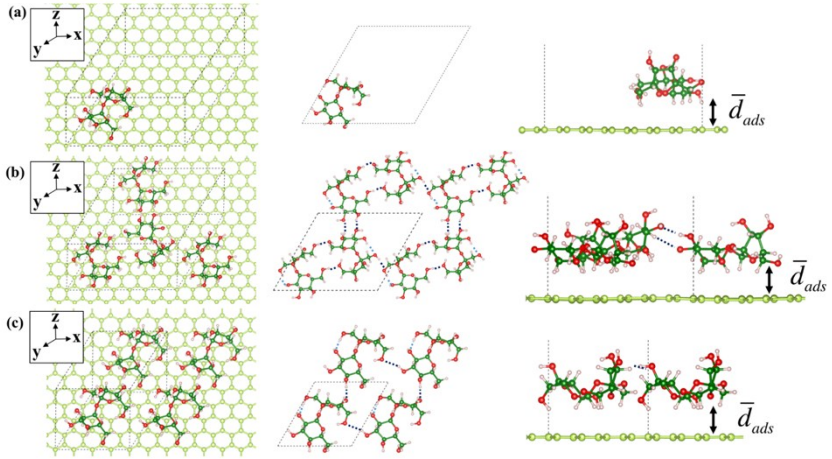

Fig. S1. (a) Isolated molecule of sucrose on graphene (right); (b) Loose supramolecular network of sucrose on graphene; (c) Compact supramolecular network of sucrose on graphene. View corresponds to perspective (right), topside view (from z axis, on centre), lateral view (from x axis, left). *Colour code*: carbon graphene (light green), carbon carbohydrate (dark green), nitrogen (light blue), oxygen (red) and hydrogen (light pink).

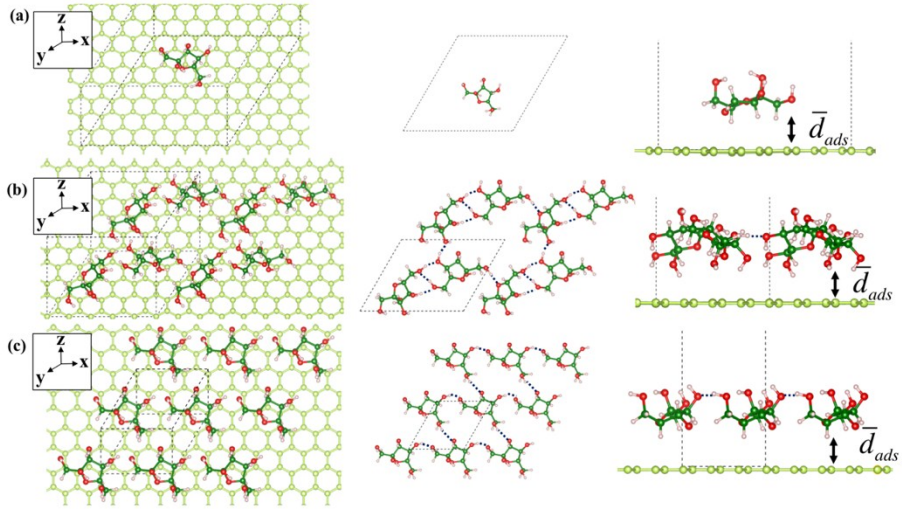

Fig. S2. (a) Isolated molecule of fructose on graphene (right); (b) Loose supramolecular network of fructose on graphene; (c) Compact supramolecular network of fructose on graphene. View corresponds to perspective (right), topside view (from z axis, on centred), lateral view (from x axis, left). *Colour code*: carbon graphene (light green), carbon carbohydrate (dark green), nitrogen (light blue), oxygen (red) and hydrogen (light pink).

Table S1. Binding energies (eV) decomposition on the supramolecular network of carbohydrates on graphene and d_{ads} (Å) average distance between carbohydrate and graphene layer.

Entry		$E_{G\text{-}SWE}$	$E_{G\text{-}dist}$	E_{SWEnet}	$E_{ads\text{-}SWE}$	d_{ads} (Å)
Isolated	Sucrose	-0.97	0.41	0.01	-0.55	4.41
	Glucose	-0.53	0.40	0.01	-0.12	4.16
	Fructose	-0.54	0.41	0.01	-0.12	3.98
Loose Network	Sucrose	-1.58	0.32	-0.78	-2.04	4.60
	Glucose	-0.65	0.15	-1.49	-2.00	5.01
	Fructose	-0.75	0.15	-1.22	-1.83	4.73
Compact Network	Sucrose	-0.84	0.10	-0.51	-1.25	4.42
	Glucose	-0.39	0.08	-0.56	-0.87	4.42
	Fructose	-0.41	0.09	-0.68	-1.01	4.24

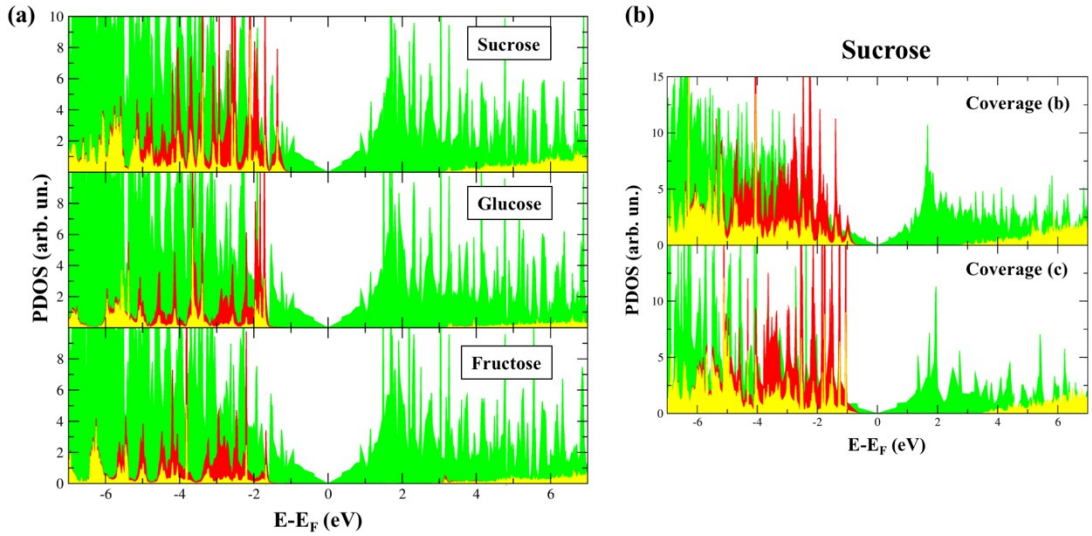

Fig. S3. (a) PDOS at PBE level for the isolated carbohydrates on graphene. (b) PDOS at PBE level for the supramolecular networks (coverage b and c) of sucrose on graphene. *Colour code:* carbon graphene (green), carbon carbohydrates (yellow), oxygen (red), For visualization purposes, the contributions from the inner s orbitals have been omitted.

Synthesis of FLG

Preparation of FLG under Neat conditions

The synthesis of FLG through mechanochemical methods initiates using graphite obtained from Bay Carbon as precursor material. D-glucose, D-fructose and sucrose were used as the exfoliating agents and were purchased from Panreac and Sigma-Aldrich. In a typical experiment for the neat conditions, graphite (75 mg) and glucose (4.5g) were placed in a 250mL stainless steel jar containing 15 stainless steel balls (2cm in diameter each). The jar was inserted in the planetary ball-milling machine (Retsch pm100) and the procedure was carried out at room temperature and air atmosphere for 2 or 4h. After the milling treatment, the resulting solid mixtures were dispersed in 100mL of water. After, these dispersions were centrifuged at 1500 rpm for 15 min to remove non-exfoliated graphite and some of the glucose. The precipitate is removed and rejected. The resulting dispersions were dialyzed to further remove the glucose in the media. The procedure consists in changing periodically the washing water while heating at 70ºC. It consists in one-over-night change and 7 changes every 90 min during the following day. The resulting dispersions were left to rest for 5 days, keeping the resulting as stable dispersions at room temperature and air atmosphere. The supernatant and the precipitate were labeled as **FLG1** and **FLG2**, respectively. Dry powder samples are obtained after lyophilisation at −80 °C at a pressure of 0.005 bar.

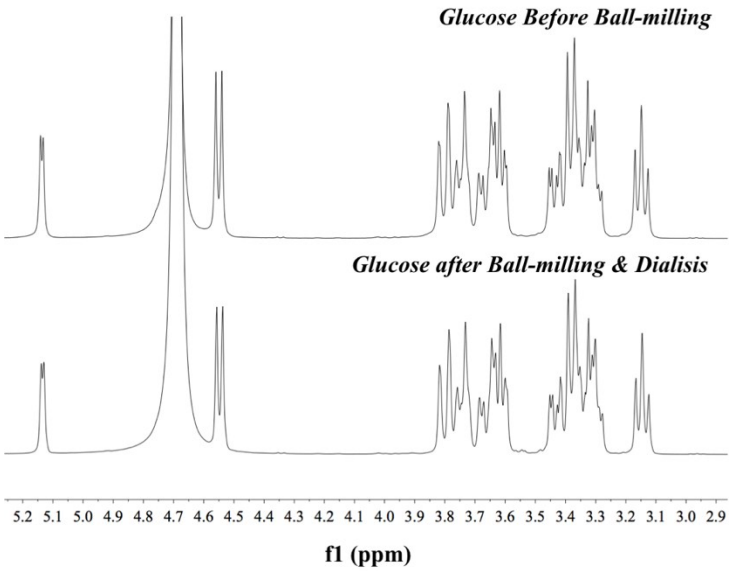

Figure S4. NMR of glucose before and after the exfoliation process and the cleaning procedure.

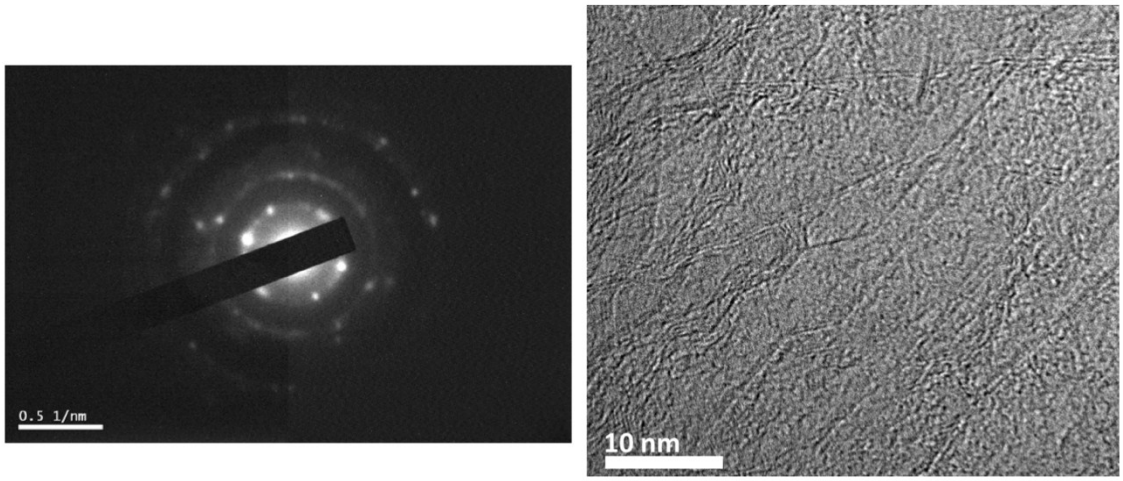

Fig. S5. SAED pattern (left) and HRTEM photos (right) of FLG obtained under Neat 4h conditions.

Preparation of Cocrystals Glucose-FLG under LAG conditions

In a typical experiment for the neat 4h conditions, graphite (75 mg), glucose (4.5g) and 2.5mL of mili-Q water were placed in a 250mL stainless steel jar containing 15 stainless steel balls (2cm in diameter each). The jar was inserted in the planetary ball-milling machine (Retsch pm100) and the procedure was carried out at room temperature and air atmosphere for 2 or 4h. After the milling treatment, the resulting solid mixtures were dispersed in 100mL of water. These dispersions were centrifuged at 1500 rpm 15 min to remove non-exfoliated graphite and some of the glucose. The precipitate is removed and discarded. Cocrystal dry powder were obtained after lyophilisation of the supernatant at −80 °C at a pressure of 0.005 bar.

Structural determination of N_G through Raman spectroscopy

Additional Raman analysis is achieved by obtaining the N_G (number of layers) of the sample. It is commonly accepted that the thickness of FLG is reflected in the shapes of the 2D Raman bands (around 2700 cm^{-1}). Following the results from Coleman and col.,[1] we calculated the N_G in our samples. The number is calculated from comparison with the Raman spectrum of the starting graphite material. We applied the following equation:

$$N_G = 10^{0.84M + 0.45M^2}$$

Where M is equal to:

$$M = \frac{I_{2Dene}(\omega = \omega_{p,\,2Dite})/I_{2Dene}(\omega = \omega_{s,\,2Dite})}{I_{2Dite}(\omega = \omega_{p,\,2Dite})/I_{2Dite}(\omega = \omega_{s,\,2Dite})}$$

Where I_{2Dene} and I_{2Dite} correspond with the intensity of 2D band for graphene and graphite, respectively. We have analyzed at least 30 individual Raman spectra of few-layer graphene of dry powder. Raman results suggest that our few-layer graphene consists of flakes with an average thickness of 2-3 layers.[2, 3]

Table S2. Average values for the intensity of the 2D band at the wavelength associated with the peak of graphite ($I_{2D,\omega p}$) and at the wavelength associated with the low energy shoulder of the graphite 2D band ($I_{2D,\omega s}$) for graphite and FLG in dry powder. Number of layers (N_G) for FLG.

Samples	Band @ 2723.35 cm^{-1} ($I_{2D,\omega p}$)	Band @ 2683.40 cm^{-1} ($I_{2D,\omega s}$)	Relation $I_{2D,\omega p}$ / $I_{2D,\omega s}$	M	N_G
Graphite	0.47	0.25	1.88	1	--
Neat 2h	0.39	0.50	0.79	0.42	2.71
Neat 4h	0.24	0.35	0.69	0.37	2.36
LAG 2h	0.40	0.55	0.73	0.39	2.50
LAG 4h	0.45	0.42	1.08	0.57	4.27

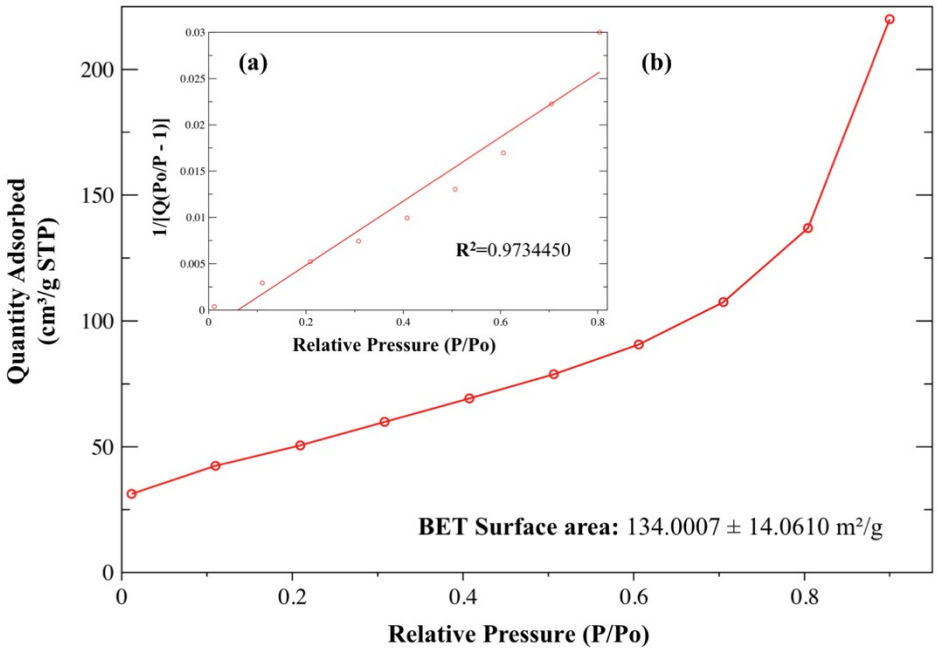

Fig. S6. (a) nitrogen adsorption plot and (b) Brunauer–Emmett–Teller (BET) surface area plot.

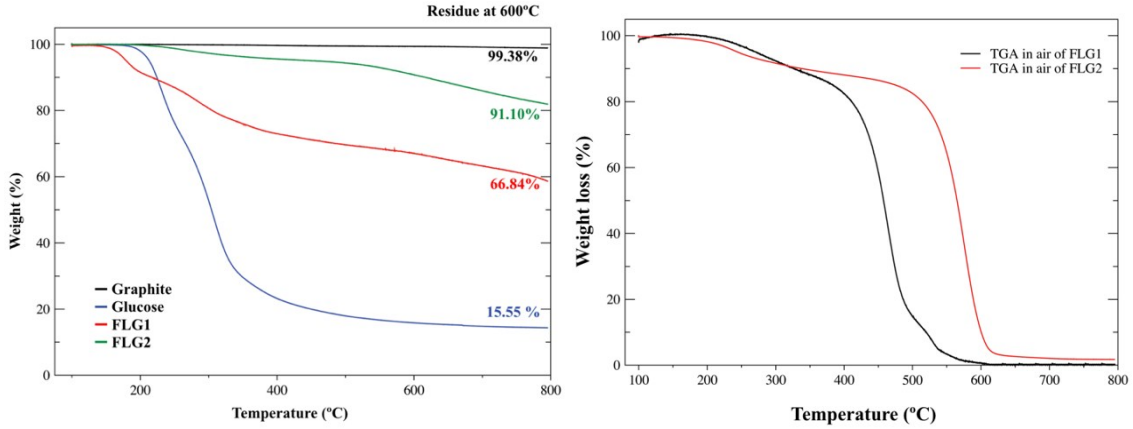

Fig. S7. (left) TGA in nitrogen results for FLG1 and FLG2 from Neat 4h samples compared with graphite and glucose; (right) TGA in air results for FLG1 and FLG2.

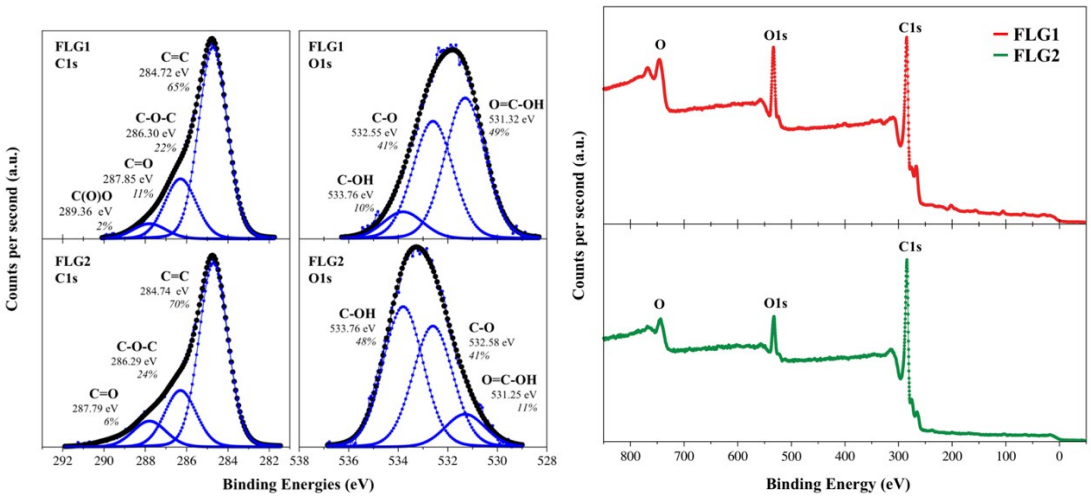

Fig. S8. (left) XPS results for FLG1 and FLG2 from the exfoliation with glucose; (right) Wide scan XPS spectra for the FLG1 and FLG2 samples.

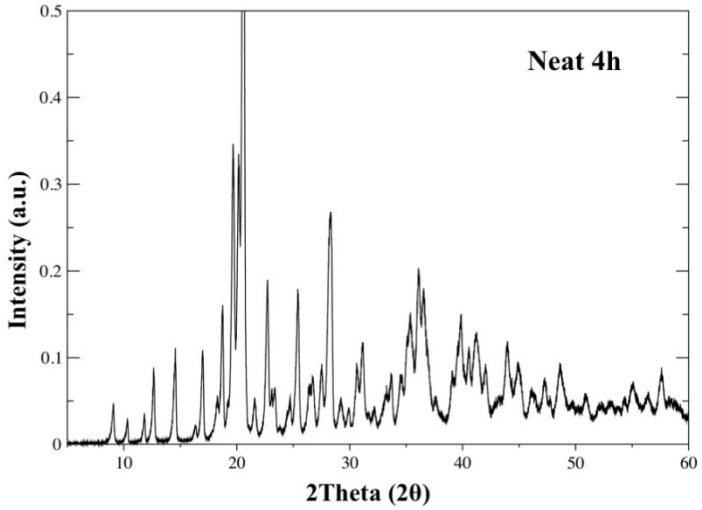

Fig. S9. Powder X-Ray diffraction (PXRD) results for Neat 4h sample. The results are normalised to the highest peak.

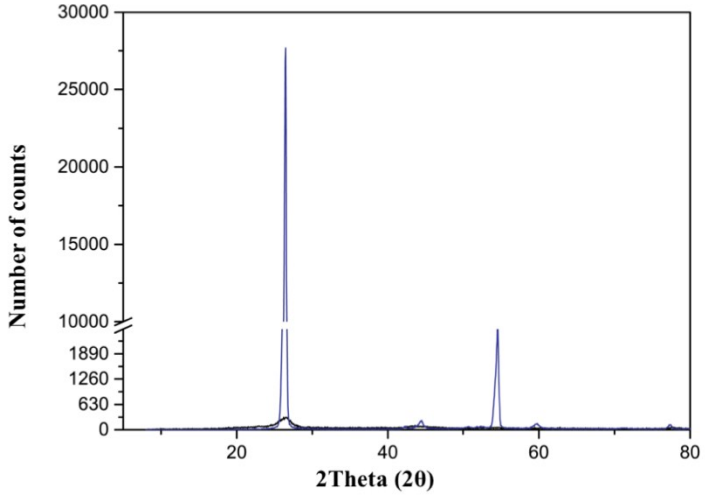

Fig. S10. Powder X-Ray diffraction (PXRD) comparison between graphite (black) and graphene (blue). The results are not normalised, they represent the real counts of intensity of each peak.

Determination of graphene through UV

The concentration of graphene is determined through the UV measurement (acquired at 660 nm) with known concentration of graphene in water media. The results render a calibration curve presented Fig. S4.

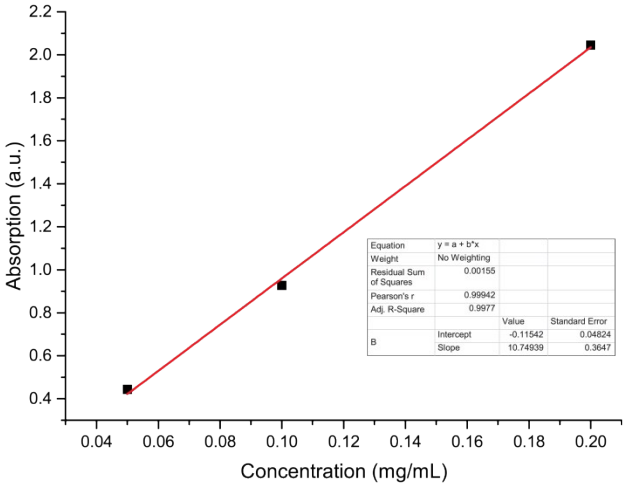

Fig. S11. UV calibration curve in the determination of graphene.

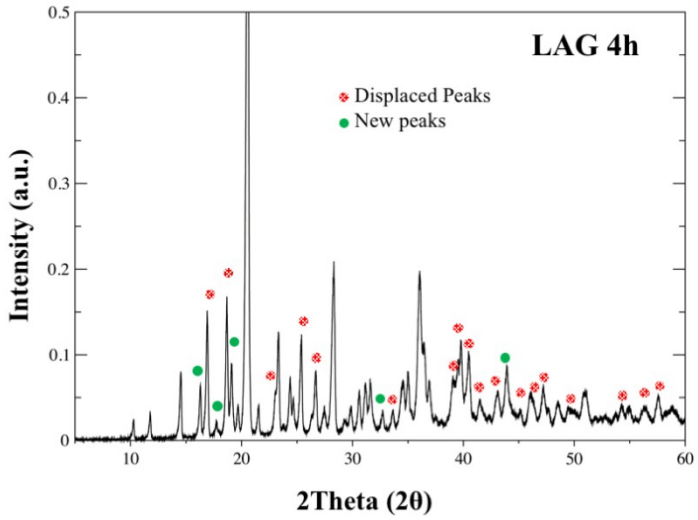

Fig. S12. Powder X-Ray diffraction (PXRD) results for LAG 4h sample. The results are normalised to the highest peak.

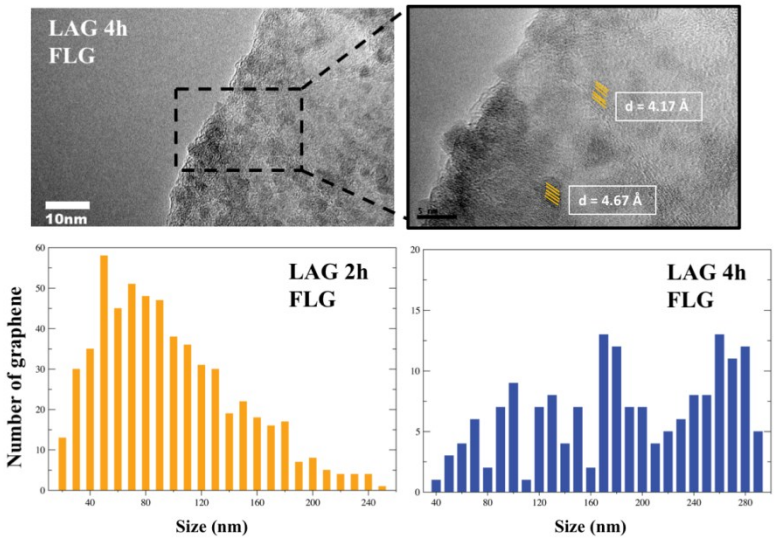

Fig. S13. TEM image and size distribution of graphene from LAG 2h and LAG 4h samples after lyophilisation.

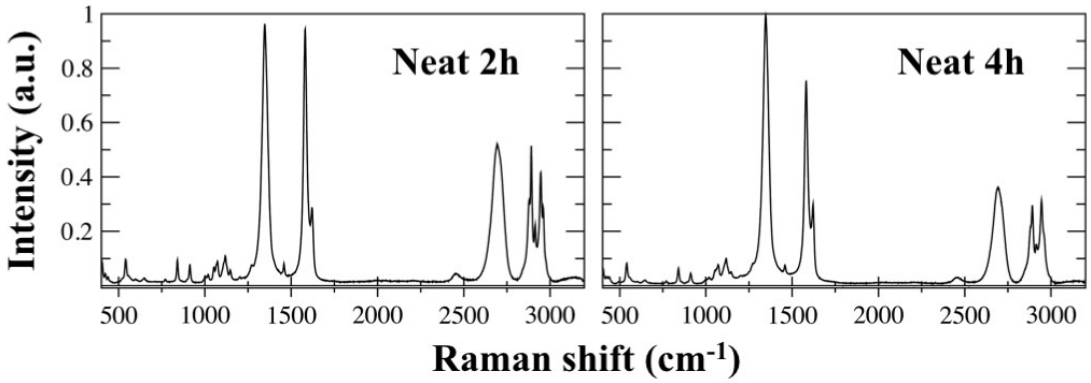

Fig. S14. Raman results for Neat 2h and Neat 4h condition.

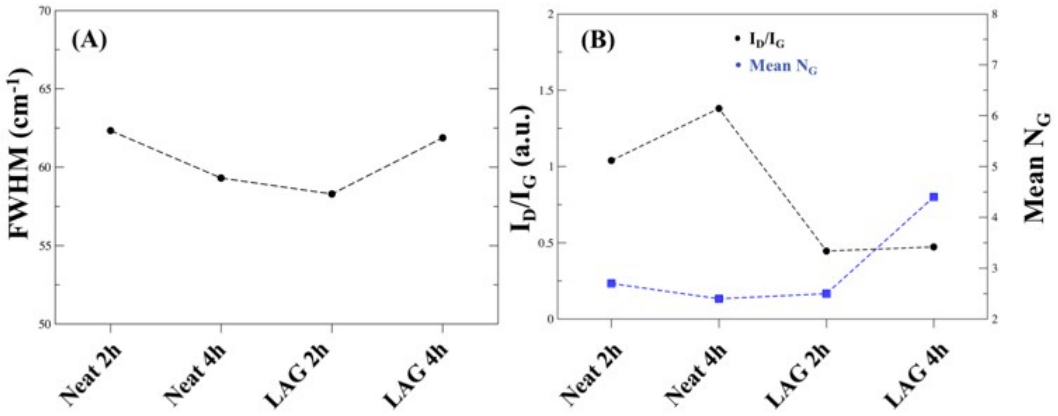

Fig. S15. FWHM values of 2D band of graphene in cocrystals under neat and LAG grinding conditions from Raman spectra.

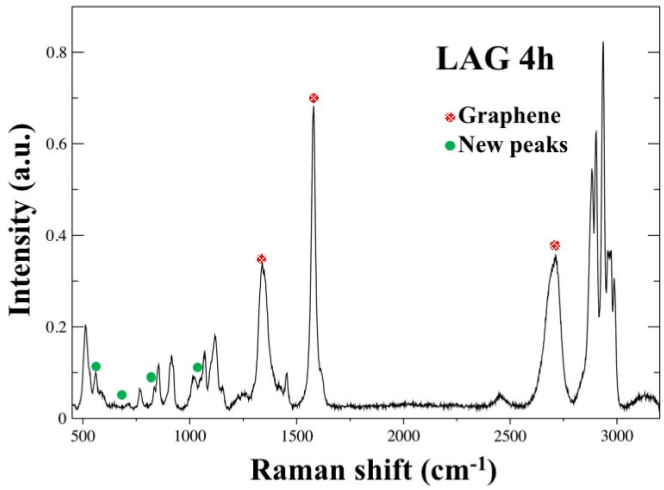

Fig. S16. Raman results for LAG 4h condition.

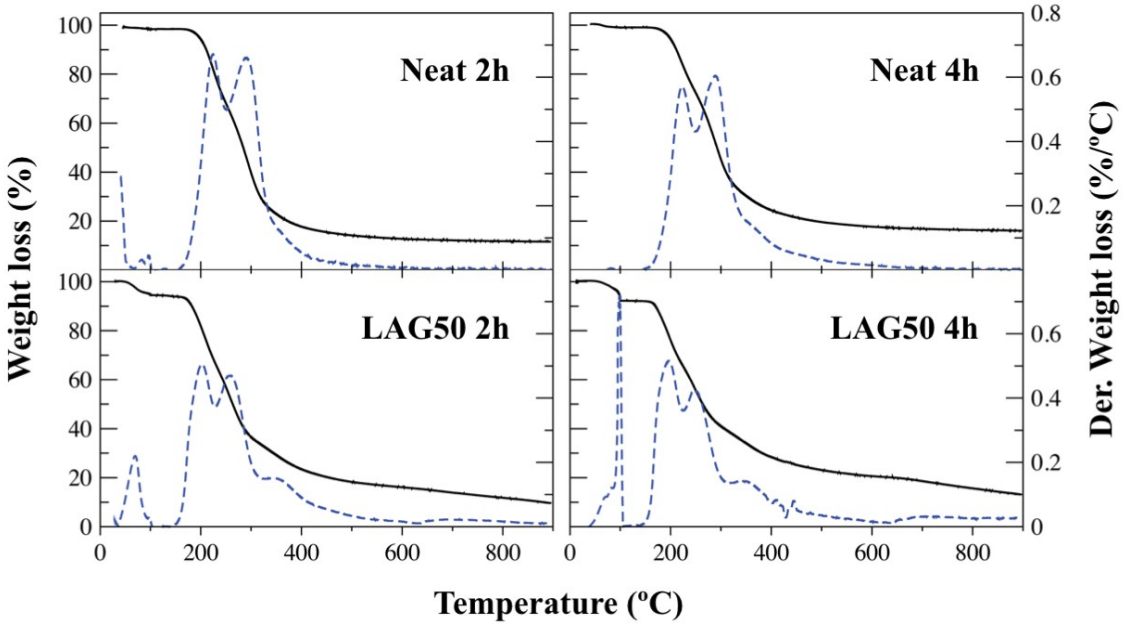

Fig. S17. TGA analysis of the neat and LAG samples

References

1. K. R. Paton, E. Varrla, C. Backes, R. J. Smith, U. Khan, A. O'Neill, C. Boland, M. Lotya, O. M. Istrate, P. King, T. Higgins, S. Barwich, P. May, P. Puczkarski, I. Ahmed, M. Moebius, H. Pettersson, E. Long, J. Coelho, S. E. O'Brien, E. K. McGuire, B. M. Sanchez, G. S. Duesberg, N. McEvoy, T. J. Pennycook, C. Downing, A. Crossley, V. Nicolosi and J. N. Coleman, *Nat. Mater.*, 2014, **13**, 624-630.
2. V. León, A. M. Rodríguez, P. Prieto, M. Prato and E. Vazquez, *ACS Nano*, 2014, **8**, 563-571.
3. V. León, M. Quintana, M. A. Herrero, J. L. G. Fierro, A. de la Hoz, M. Prato and E. Vázquez, *Chem. Commun.*, 2011, **47**, 10936-10938.